ChemComm

Accepted Manuscript

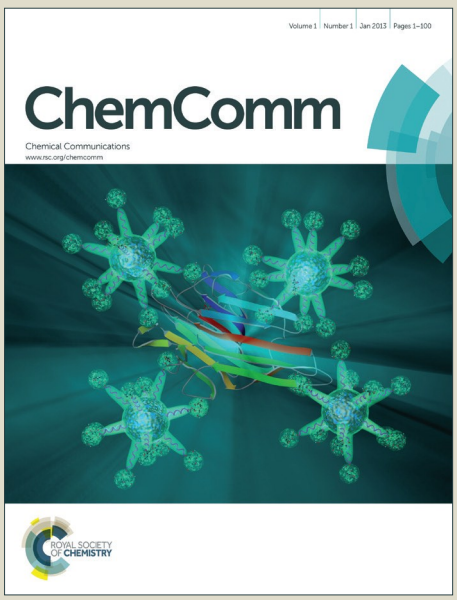

ROYAL SOCIETY OF CHEMISTRY

www.rsc.org/chemcomm

Journal Name

Communication

Self-Assembled Nanofiber Hydrogels for Mechanoresponsive Therapeutic Anti-TNFα Antibody Delivery

Received 00th January 20xx,
Accepted 00th January 20xx

DOI: 10.1039/x0xx00000x

www.rsc.org/

J. A. Kaplan,[a] P. Barthélémy[b] and M. W. Grinstaff[a†]

Low molecular weight hydrogels, prepared from glycosyl-nucleoside-lipid amphiphiles, exhibit shear-thinning behaviour and reversible thermally- and mechanically-triggered sol-gel transitions. Using mechanical shear stimulation, the release of entrapped anti-TNFα increases and the released anti-TNFα demonstrates efficacy in *in vitro* neutralization bioassays. Delivery of anti-TNFα is of general interest and broad medicinal utility for treating autoimmune diseases such as rheumatoid arthritis.

Hydrogels are of interest across a broad range of biomedical activities including drug delivery, high throughput screening, tissue engineering, and wound-healing.[1-12] Traditionally, hydrogels are prepared from large molecular weight macromolecules (>5,000 g/mol) via physical entanglements or chemical crosslinking of the constituents. More recently, the principles of supramolecular chemistry[13] are being exploited to prepare small molecules that self-assemble into higher-order functional structures, affording hydrogels,[14-18] including those that are stimuli-responsive[19, 20] and/or self-healing.[21, 22] Often the low molecular weight (LMW) gelators used to form these supramolecular systems possess biologically important chemical structures including peptides,[18, 23, 24] carbohydrates,[25, 26] or nucleosides.[27, 28]

From a chemical perspective, LMW gelators that spontaneously form hydrogels in aqueous environments are of interest for drug and nucleic acid delivery, and for cell and tissue engineering scaffolds.[11, 29-31] GNL hydrogels implanted subcutaneously are stable for more than two months.[32] Moreover, the macroscopic reversibility or self-healing characteristics of these hydrogels provides an opportunity to design and evaluate mechanoresponsive materials for drug delivery. Therefore, the goal of this work is to synthesize a low molecular weight hydrogel composed of a sugar, nucleoside, and fatty acid subunit, study its rheological properties, and investigate the potential of this hydrogel for shear-mediated release of an entrapped biologic. Mechanoresponsive biomaterials[33, 34] for the controlled delivery of growth factors[35] and other therapeutics[36-38] is an active area of research, and the shear-mediated approach described herein is unique from the previous studies, as well as uses a LMW gelator composed of biocompatible building blocks. Specifically, we report the: 1) synthesis of an oleoylamide glycosyl-nucleoside-lipid (GNL) gelator; 2) formation of hydrogels through an entangled, self-assembled nanofiber network; 3) exhibition of hydrogel shear-thinning, creep/recovery, thermo- and mechano-reversible behaviour; 4) diffusion of FITC-dextrans as model biopolymers; 5) shear-mediated release of 166 kDa FITC-dextran and an IgG directed against human TNFα, serving as a biopharmaceutical example; and 6) efficacy of this mechanoresponsive anti-TNFα delivery strategy in an *in vitro* cytokine neutralization assay.

The oleoylamide GNL (Fig. 1a) was prepared according to

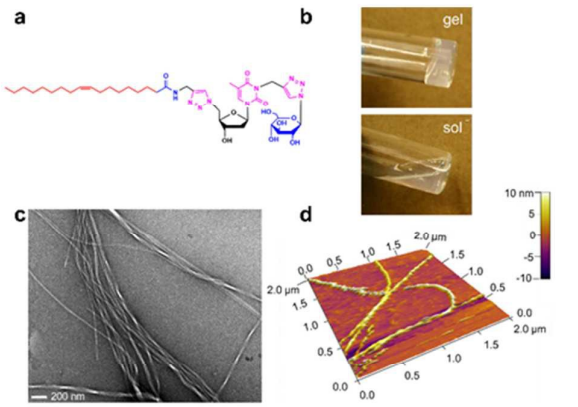

Fig. 1. (a) Chemical structure of the oleoylamide glycosyl-nucleoside-lipid (GNL) highlighting the non-covalent interactions of each part of the amphiphile structure: hydrophobic (red), hydrogen-bonding (blue), and pi-stacking (pink). (b) Photograph of GNL hydrogel at 23 °C (top) and sol at 60 °C (bottom), which is above the gel-sol transition. (c) TEM image of fibres formed from dilute GNL in aqueous solution. (d) AFM image of hydrogel (height profile), showing a bundle of GNL fibres.

[a] Departments of Biomedical Engineering and Chemistry, Boston University, Boston, Massachusetts 02215
[b] Inserm, U869, Bordeaux, F-33076 France, Université de Bordeaux, F-33076, Bordeaux, France.
† Corresponding Author. E-mail: mgrin@bu.edu

Electronic Supplementary Information (ESI) available: Synthesis and characterization data for GNL gelator amphiphiles; FRAP, rotational shear rheometry, and *in vitro* cell assay protocols. See DOI: 10.1039/x0xx00000x

our earlier reports[16, 39] with minor modifications, and the complete synthetic details, including analysis, are found in the Supplementary Information (SI, Fig. S1, available online). Upon heating and subsequent cooling, the GNLs self-assemble to form clear hydrogels in aqueous media (4 wt%, Fig. 1b) through non-covalent intermolecular forces, which include: hydrophobic interactions among the hydrocarbon chains; π-stacking of the nucleoside and triazole bridges; and hydrogen bonding among the thymidine, triazole, amide, and glucopyranoside moieties. Each component of this amphiphile structure is required to form the hydrogel.[38] TEM experiments reveal the origin of the hydrogel as an intertwined network of ~12 nm diameter nanofibers (Fig. 1c), and are in agreement with atomic force microscopy studies of GNL hydrogels deposited on mica, showing ~11 nm-diameter fibres (Fig. 1d).

We measured the viscoelastic properties of GNL hydrogels as a function of temperature, frequency, and stress/strain amplitude using rotational shear rheometry. In order to elucidate the direct effects each parameter has on a material's response, the linear viscoelastic region (LVR) was first determined using an oscillatory stress sweep at 1.0 Hz and 37 °C. Within this regime, the elastic storage modulus (G') and viscous loss modulus (G'') were ~20 and 2 Pa, respectively (see Fig. S2). The yield stress occurred at 13.7 ± 1.9 Pa, while the flow point (or critical yield stress) of the gel occurred at 27.3 ± 3.8 Pa. The frequency sweep study involved oscillations over the range of 0.1 to 100 Hz; however, due to the weak nature of the hydrogel, only meaningful data were obtained from 0.1 to 10 Hz (Fig. 2a) before inertial effects (characterized by a raw phase angle ≥150 degrees for our instrument) dominated the signal. Shear rate-dependent behaviour was observed for this hydrogel, as complex viscosity $|\eta^*|$ decreases from 20 to 0.4 Pa·s with increasing shear rate/frequency. The GNL hydrogel can be delivered through a small 21G needle. Additionally, viscoelastic creep and recovery were observed on the time-scale of seconds using a 0.1 Pa applied stress (Fig. 2b). Repeated attempts to perform a similar experiment using 10 Pa applied stress were unsuccessful due to adverse inertial effects from creep ringing (creep ringing is seen at ~60 seconds in Fig. 2b and magnified image is shown in Fig. S3).[40]

Temperature-dependent mechanics and thermal reversibility of the GNL hydrogel (G', G'', and δ) were investigated using a temperature sweep from 37 °C to 58 °C, and then down to 10 °C at constant rates of ± 1.0 °C/min, respectively. The data presented in Fig. 2c indicated thermal reversibility for these hydrogels. A clear sol-gel transition was observed at ~58 °C, although δ begins to noticeably increase at temperatures ≥45 °C. The macroscopic reversibility of these hydrogels was further determined by subjecting samples to three small- medium- and large-amplitude oscillatory shear cycles (Fig. 2d) wherein increasing oscillatory stress values (1 Pa, 10 Pa, and 100 Pa) were sequentially applied, with 2-min rests in between. The tests were repeated twice more on the same hydrogels, for a total of 3 cycles. Values for δ reversibly fluctuated from ~10 to >60 degrees as the network ruptured and reformed. The return to a hydrogel state occurred relatively fast, within <2 minutes, and there was no statistical change in mechanical response between the first and third cycle (p= 0.53 and p = 0.11 for 5 Pa and 100 Pa applied stress, respectively).

To characterize the diffusion of biomacromolecules within the GNL hydrogels, the diffusivity coefficients of entrapped fluorescein isothiocyanate (FITC)-labelled dextrans were determined by fluorescence recovery after photobleaching (FRAP). Using confocal microscopy, fluorescence time-series micrographs of FITC-dextrans (19.6 kDa, 39 kDa, and 167 kDa) loaded at 0.5 mg/mL in the GNL hydrogel were acquired before and after photobleaching a 100-μm diameter region of interest. The average percent recovery curves after photobleaching for the three different MW dextrans, and the

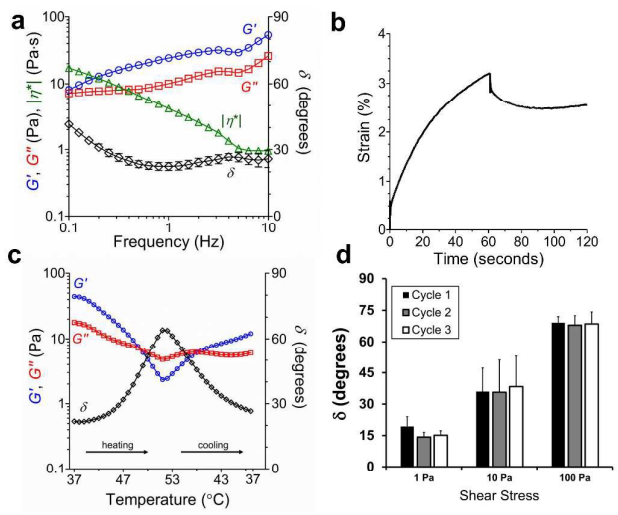

Fig. 2. (a) Frequency sweep of GNL hydrogel (τ = 10 Pa, 37 °C). (b) Creep curve for a 40 mg/mL hydrogel under 0.1 Pa applied stress, and subsequent recovery after removal of shear stress. (c) Temperature sweep (f = 1.0 Hz, τ = 10 Pa) of GNL hydrogel. (d) Cyclic reversibility tests on hydrogels wherein the samples experience alternating small-, medium- and large-amplitude oscillatory shear stress, recovering their original mechanical properties after each cycle (~2 min). Error bars represent ±SD for triplicate samples.

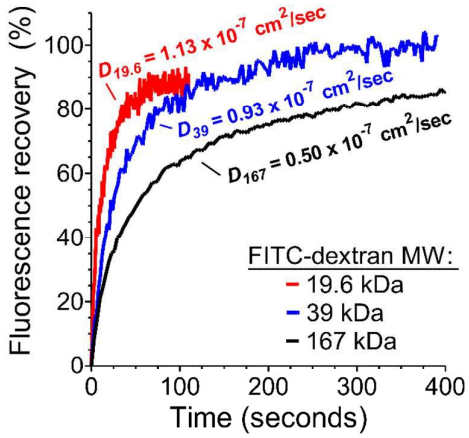

Figure 3. Fluorescence recovery after photobleaching (FRAP) of FITC-dextrans. Diffusion coefficients (D) are listed next to their respective FRAP curves.

diffusion coefficients (calculated using a MATLAB program based off the work of Jain et al.[41]), are 1.13, 0.93, and 0.50 x 10^{-7} cm^2/sec, respectively. The smallest molecular weight FITC-dextran (19.6 kDa) had the largest diffusion coefficient approximately 2.3× that of the largest FITC-dextran (167 kDa) tested (Fig. 3).

Due to the soft and reversible nature of the hydrogel, we hypothesized that shearing (i.e., rupturing the physical crosslinks) may influence the release rate of a large molecular weight (MW = 167 kDa) FITC-dextran (Fig. 4a). A shear value of 10 Pa was selected based on our initial stress sweep data, which provided adequate stress to disrupt the gel and nanofiber crosslinks, based on the yield stresses identified. A statistically significant increased release of the 167 kDa FITC-dextran from GNL hydrogels was observed under 10 Pa shear compared to hydrogels at rest (Fig. 4b).

The above data showing GNL hydrogels form under mild gelation conditions, are able to release biomacromolecules under applied shear stress, and permit molecular weight-dependent diffusion throughout the matrix suggests their ability to act as mechanically-controlled delivery depots for therapeutic proteins such as enzymes and antibodies. Thus, we studied shear-mediated macromolecule release using a rabbit immunoglobulin G (IgG) antibody (~150 kDa) directed against human TNFα (Fig. 4). Anti-TNFα was chosen as the model antibody in this study because of its broad clinical utility as an anti-inflammatory agent ("TNF blocker"), such as in treating rheumatoid arthritis.[42, 43] Moreover, the availability of several cell lines with sensitivity to TNFα in the pg/mL range have allowed facile, reproducible, and sensitive measurements of both TNFα concentrations and the *in vitro* efficacy of anti-TNFα therapy using a corresponding cytokine neutralization assay.[44, 45] Release aliquots of anti-TNFα from GNL hydrogels in the presence or absence of shear were assessed for their ability to neutralize the cytotoxicity of human TNFα (IC_{50} = 51 pg/mL, Fig. S4) in the L929 murine fibroblast cell line. Without application of shear for both hydrogel samples (0 minute time point), TNFα release is minimal and not statistically different between the two samples (p >0.05; Figure 4c). The GNL hydrogels experiencing 10 Pa shear neutralized (i.e., reduced) TNFα toxicity by ~60% after 90 minutes, compared to ~10% neutralization of non-sheared antibody-loaded hydrogels (Fig. 4c). The relative release of anti-TNFα for sheared and non-sheared samples was ~20% and ~7.5%, respectively, which were determined by comparing to a previously constructed TNFα neutralization curve performed with known concentrations of antibody (Fig. S5). Our working hypothesis is that the release of the anti-TNFα from the hydrogel is attributed to temporary loss of the hydrogel structure (with return to a low viscous aqueous solution) upon shearing via disassembly of the GNL supramolecular nanofibers.

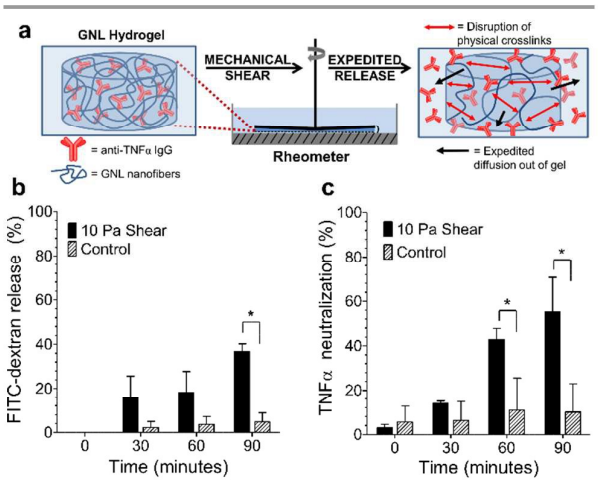

Fig. 4. (a) Schematic diagram of shear-mediated release using a rheometer. Entrapped macromolecules, shown as "Y" in the figure, are slow to diffuse out into a water bath (light blue) due to the presence of GNL nanofiber entanglements (blue lines). (b,c) The diffusion of 167 kDa FITC-dextran (b) and rabbit anti-human TNFα IgG (c) from within GNL hydrogels into the surrounding environment is increased with 10 Pa applied oscillatory shear stress, resulting in neutralization of TNFα cytotoxic activity in a L929 bioassay.

The hydrogel state, viscoelasticity, and observed mechanical properties arise from the entanglement of nanofibers assembled from individual GNL molecules. Dynamic stress sweeps reveal a linear viscoelastic region, followed by a deviation of the linear stress-strain relationship before gel rupture at the flow point. Data collected as a function of amplitude, temperature, and frequency show predictable and reversible sol-gel transitions, and cyclic reversibility tests (i.e., gel rupture and reformation) demonstrate the reversibility of these supramolecular assemblies. Finally, these entangled nanofiber assemblies impede the diffusion of macromolecules within the gel matrix in a molecular weight-dependent fashion, yet may be mechanically stressed to facilitate diffusion into the surrounding environment to elicit biological activity *in vitro*. These results highlight the utility of using supramolecular principles to create macroscopic functional materials, such as hydrogels, which may entrap delicate and bioactive substances for subsequent delivery,[46] since the conditions for gel formation (and rupture) are mild, yet tuneable along with a hydrogel that can be easily administered via a small-gauge needle. The use of LMW gelators for preparing mechanoresponsive hydrogels represents a unique approach that complements previous systems—for example, those employing crosslinked polymers. Continued research in this area will afford new compositions of low molecular weight gelators and materials, as well as reveal structure-property relationships to aid in the design of application-specific materials for protein delivery.

Notes and references

We thank Nitinun 'Bell' Varongchayakul for assistance with AFM studies, Dr. Guilhem Godeau for useful discussions and TEM imaging on the GNLs, and Dr. Philip Allen of the Micro/Nano Imaging Facility at Boston University for his assistance with confocal microscopy. MATLAB code for importing, analyzing, and calculating the diffusion coefficient was generously provided by Dr. Steven Meyers. This work was supported by Boston University. P.B. acknowledges financial support from the French National Agency

(ANR) in the frame of its programme blanc (project GelCells, appel à projets Blanc SIMI 7-2010).

1. T. Billiet, M. Vandenhaute, J. Schelfhout, S. Van Vlierberghe and P. Dubruel, *Biomaterials*, 2012, **33**, 6020-6041.
2. J. A. Burdick and K. S. Anseth, *Biomaterials*, 2002, **23**, 4315-4323.
3. P. Del Gaudio, F. De Cicco, R. P. Aquino, P. Picerno, P. Russo, F. Dal Piaz, V. Bizzarro, R. Belvedere, L. Parente and A. PetrellaDepartment, *Carbohydr. Polym.*, 2015, **115**, 629-635.
4. M. M. Dominguez, M. Wathier, M. W. Grinstaff and S. E. Schaus, *Anal. Chem.*, 2007, **79**, 1064-1066.
5. C. Ghobril and M. W. Grinstaff, *Chem. Soc. Rev.*, 2015, **44**, 1820-1835.
6. A. C. Jen, M. C. Wake and A. G. Mikos, *Biotechnol. Bioeng.*, 1996, **50**, 357-364.
7. J. Kopecek, *J. Polym. Sci. A Polym. Chem.*, 2009, **47**, 5929-5946.
8. K. Y. Lee and D. J. Mooney, *Chem. Rev.*, 2001, **101**, 1869-1880.
9. C. Lin and A. T. Metters, *Adv. Drug Deliver. Rev.*, 2006, 1379-1408.
10. N. A. Peppas, J. Z. Hilt, A. Khademhosseini and R. Langer, *Adv. Mater.*, 2006, **18**, 1345-1360.
11. K. S. Straley, C. Wong Po Foo and S. C. Heilshorn, *J. Neurotraum.*, 2010, **27**, 1-19.
12. J. L. West and J. A. Hubbell, *React. Polym.*, 1995, **25**, 139-147.
13. S. Zhang, *Nat. Biotechnol.*, 2003, **21**, 1171-1178.
14. M. deLoos, B. L. Feringa and J. H. van Esch, *Eur. J. Org. Chem.*, 2005, 3615-3631.
15. J. A. Foster, M. O. M. Piepenbrock, G. O. Lloyd, N. Clarke, J. A. K. Howard and J. W. Steed, *Nature Chemistry*, 2010, **2**, 1037-1043.
16. G. Godeau and P. Barthélémy, *Langmuir*, 2009, **25**, 8447-8450.
17. A. R. Hirst, B. Escuder, J. F. Miravet and D. K. Smith, *Angew. Chem. Int. Ed. Engl.*, 2008, **47**, 8002-8018.
18. T. Suga, S. Osada, T. Narita, Y. Oishi and H. Kodama, *Mater. Sci. Eng., C*, 2015, **47**, 345-350.
19. K. S. Moon, H. J. Kim, E. Lee and M. Lee, *Angew. Chem. Int. Ed.*, 2007, **46**, 6807-6810.
20. S. C. Lange, J. Unsleber, P. Drucker, H. J. Galla, M. P. Waller and B. J. Ravoo, *Org. Biomol. Chem.*, 2015, **13**, 561-569.
21. Z. Rao, M. Inoue, M. Matsuda and T. Taguchi, *Colloids Surf. B: Biointerfaces*, 2011, **82**, 196-202.
22. A. Vidyasagar, K. Handore and K. M. Sureshan, *Angew. Chem. Int. Ed.*, 2011, **50**, 8021-8024.
23. S. Banta, I. R. Wheeldon and M. Blenner, *Ann. Rev. Biomed. Eng.*, 2010, **12**, 167-186.
24. C. Yan and D. J. Pochan, *Chem. Soc. Rev.*, 2010, **39**, 3528-3540.
25. L. S. Birchall, S. Roy, V. Jayawarna, M. Hughes, E. Irvine, G. T. Okorogheye, N. Saudi, E. De Santis, T. Tuttle, A. A. Edwards and R. V. Ulijn, *Chem. Sci.*, 2011, **2**, 1349-1355.
26. J. H. Jung, S. Shinkai and T. Shimizu, *Chem. Eur. J.*, 2002, **8**, 2684-2690.
27. K. Araki and I. Yoshikawa, *Top. Curr. Chem.*, 2005, **256**, 133-165.
28. A. Gissot, M. Camplo, M. W. Grinstaff and P. Barthelemy, *Org. Biomol. Chem.*, 2008, **6**, 1324-1333.
29. L. Haines-Butterick, K. Rajagopal, M. Branco, D. Salick, R. Rughani, M. Pilarz, M. S. Lamm, D. J. Pochan and J. P. Schneider, *Proc. Nat. Acad. Sci.*, 2007, **104**, 7791-7796.
30. L. Latxague, M. A. Ramin, A. Appavoo, P. Berto, M. Maisani, C. Ehret, O. Chassande and P. Barthélémy, *Angew. Chem. Int. Ed.*, 2015, **54**, 4517-4521.
31. M. T. McClendon and S. I. Stupp, *Biomaterials*, 2012, **33**, 5713-5722.
32. S. Ziane, S. Schlaubitz, S. Miraux, A. Patwa, C. Lalande, I. Bilem, S. Lepreux, B. Rousseau, J.-F. Le Meins, L. Latxague, P. Barthélémy and O. Chassande, *European Cells and Materials*, 2012, **23**, 147-160.
33. B. D. Riehl, J. H. Park, I. K. Kwon and J. Y. Lim, *Tissue Eng. Part B Rev.*, 2012, **18**, 288-300.
34. Y. Yang, J. L. Magnay, L. Cooling and A. J. El Haj, *Biomaterials*, 2002, **23**, 2119-2126.
35. K. Y. Lee, M. C. Peters, K. W. Anderson and D. J. Mooney, *Nature*, 2000, **408**, 998-1000.
36. N. Korin, M. Kanapathipillai, B. D. Matthews, M. Crescente, A. Brill, T. Mammoto, K. Ghosh, S. Jurek, S. A. Bencherif, D. Bhatta, A. U. Coskun, C. L. Feldman, D. D. Wagner and D. E. Ingber, *Science*, 2012, **337**, 738-742.
37. M. N. Holme, I. A. Fedotenko, D. Abegg, J. Althaus, L. Babel, F. Favarger, R. Reiter, R. Tanasescu, P.-L. Zaffalon, A. Ziegler, B. Muller, T. Saxer and A. Zumbuehl, *Nature Nanotechnology*, 2012, **7**, 536-543.
38. T. Saxer, A. Zumbuehl and B. Muller, *Cardiovasc. Res.*, 2013, **99**, 328-333.
39. G. Godeau, J. Bernard, C. Staedel and P. Barthelemy, *Chem. Commun.*, 2009, DOI: 10.1039/B906212B, 5127-5129.
40. R. H. Ewoldt and G. H. McKinley, *Rheology Bulletin*, 2007, **76**, 4-24.
41. R. K. Jain, R. J. Stock, S. R. Chary and M. Rueter, *Microvasc. Res.*, 1990, **39**, 77-93.
42. G. R. Burmester, R. Panaccione, K. B. Gordon, M. J. McIlraith and A. P. M. Lacerda, *Ann. Rheum. Dis.*, 2013, **72**, 517-524.
43. M. Feldmann, *Nat. Rev. Immunol.*, 2002, **2**, 364-371.
44. W.-C. Chiu, Y.-P. Lai and M.-Y. Chou, *PloS one*, 2011, **6**, e16373.
45. M. Y. Shiau, H. L. Chiou, Y. L. Lee, T. M. Kuo and Y. H. Chang, *Mediators Inflamm.*, 2001, **10**, 199-208.
46. N. A. Peppas, K. M. Wood and J. O. Blanchette, *Expert Opin. Biol. Ther.*, 2004, **4**, 881-887.

TOC Graphic